Available online at www.sciencedirect.com

ScienceDirect

Energy Procedia 55 (2014) 265 – 271

Energy Procedia

4th International Conference on Silicon Photovoltaics, SiliconPV 2014

# Ion implantation for all-alumina IBC solar cells with floating emitter

Ralph Müller[a,]*, Christian Reichel[a], Jan Benick[a], Martin Hermle[a]

[a]*Fraunhofer Institute for Solar Energy Systems (ISE), Heidenhofstrasse 2, D-79110 Freiburg, Germany*

**Abstract**

Interdigitated back contact (IBC) solar cells have a high efficiency potential. However, the fabrication of this cell structure is quite complex. Ion implantation for structured doping together with batch reactors for front and rear side passivation with $Al_2O_3$ could help to reduce the fabrication effort. Since $Al_2O_3$ gives a very good passivation on *p*-doped surfaces, we investigate *n*-type IBC solar cells with a low-dose ion-implanted front floating emitter (FFE) which we compare to a low-dose ion implanted front surface field (FSF) passivated by $SiO_2$. We measured saturation current densities ($J_0$) between 10 and 15 fA/cm$^2$ for the $SiO_2$ passivated FSF and down to 5 fA/cm$^2$ for the $Al_2O_3$ passivated FFE on textured samples. The FFE has been successfully applied to fully implanted IBC cells ($\eta = 21.8$ %). Cells with FSF degraded strongly under UV-illumination due to the instable $SiO_2$ passivation on the front side while the FFE cells with $Al_2O_3$ passivation were much less affected. IV measurements under low level illumination revealed a linear performance down to 0.01 suns for both, FSF and FFE.

© 2014 The Authors. Published by Elsevier Ltd. This is an open access article under the CC BY-NC-ND license (http://creativecommons.org/licenses/by-nc-nd/3.0/).
Peer-review under responsibility of the scientific committee of the SiliconPV 2014 conference

*Keywords:* ion implantation; IBC solar cells; floating emitter

## 1. Introduction

Interdigitated back contact (IBC) solar cells have a high efficiency potential as there are no metal contacts on the front side resulting in a maximum absorption of the incident light. Having both, *n*- and *p*-contacts, on the back side necessitates a structured doping which makes the fabrication of this cell concept quite complex. It has been shown

* Corresponding author. Tel.: +49 761 4588 5921; fax: +49 761 4588 9250.
*E-mail address:* ralph.mueller@ise.fraunhofer.de

1876-6102 © 2014 The Authors. Published by Elsevier Ltd. This is an open access article under the CC BY-NC-ND license (http://creativecommons.org/licenses/by-nc-nd/3.0/).
Peer-review under responsibility of the scientific committee of the SiliconPV 2014 conference
doi:10.1016/j.egypro.2014.08.078

that selective doping structures can be easily formed by ion implantation using shadow masks [1]. This process could help to reduce the fabrication complexity of IBC solar cells significantly. As the IBC solar cell relies on a perfect passivation on the front side, the formation of a very lowly doped FSF or FFE which allows for a low recombination would be quite beneficial for this type of cell. Such type of profiles can easily be realized by ion implantation. Another possibility to get to a cost effective production is the passivation of both sides in a single process step using large scale ALD batch reactors. $Al_2O_3$ is an excellent passivation of (implanted) boron-doped profiles [2] and, recently, it has been shown that it is also possible to achieve a good passivation of heavily phosphorus-doped profiles applying suitable process parameters [3].

An all-alumina passivated IBC cell on *n*-type material can be realized by applying a boron-doped floating emitter on the front side. This concept could benefit from the stable passivation provided by the $Al_2O_3$ passivation [4]. It is known that the passivation quality of $SiO_2$ degrades under UV-illumination [5, 6]. Gruenbaum *et al*. found an increased surface recombination velocity after UV-illumination, most probably due to an increased defect density at the $Si/SiO_2$ interface [5]. Since alumina passivation is mainly based on the electrical shielding of electrons by the huge amount of fixed negative charges, a much weaker influence of UV-illumination on the passivation quality is expected [4]. A front floating emitter (FFE) formed with a $POCl_3$ diffusion on *p*-type material and passivated with a $SiO_2/SiN_x$ layer stack was already investigated by Granek *et al*. [7]. They found a poor cell performance compared to samples with a conventional front surface field (FSF) on *n*-type material at low illumination intensities which was explained by a defect related shunt resistance across the floating junction. It is still unclear whether this effect influences a boron-doped front floating emitter in *n*-type IBC solar cells to the same extent as phosphorus-doped front floating emitter in *p*-type IBC-solar cells.

In this study processes for the formation of doping profiles suitable for all-alumina *n*-type IBC solar cells are presented. We evaluate different processing parameters and those resulting in the most promising profiles are applied for the fabrication of small area solar cells. IBC solar cells featuring an alumina passivated floating emitter and reference cells with a FSF passivated by a $SiO_2/SiN_x$ stack were fabricated. We compared the cell performance of FSF and FFE cells under low level illumination and the degradation due to UV-illumination.

## 2. Experimental

Symmetrical lifetime samples were prepared on 10 Ω cm *n*-type FZ silicon. They first received an RCA clean followed by a boron or a phosphorus implantation (Varian VIISta HC) on both sides with doses between 1e13 and 3e15 $cm^{-2}$. Then all samples received an SC2 clean before the annealing in a tube furnace. For this process a peak time of 80 min at 1050 °C in a non-oxidizing atmosphere has been applied. For the passivation, the samples were either dipped in HF (1 % HF) and received an alumina passivation (plasma assisted atomic layer deposition, PA-ALD) or entered the furnace again to grow a 10 nm thermal oxide which then was capped by a PECVD silicon nitride. Finally, the $Al_2O_3$ and $SiO_2/SiN_x$ passivation was activated or improved by a forming gas anneal for 25 min at 425 °C, respectively.

For the fabrication of small area IBC solar cells we used 1 Ω cm *n*-type FZ silicon. The samples received an RCA clean and random pyramids were etched on the front side (only in active cell area). Ion implantation was used to form the doped regions: floating emitter (FE) on the textured front side (1e14 $cm^{-2}$ boron), emitter (1.5e15 $cm^{-2}$ boron) and back surface field (BSF) (3e15 $cm^{-2}$ phosphorus) on the planar back side. The masking of the local implantations was done by photoresists. All implanted regions were co-annealed in a tube furnace for 80 min at 1050 °C in a non-oxidizing atmosphere and passivated by PA-ALD $Al_2O_3$. The front side was capped by a PECVD nitride and the back side by a PECVD silicon oxide. Aluminum was evaporated on the back side (10 µm thickness) and structured in a wet chemical etch solution with a photoresist mask. Finally, the finished cells were annealed on a hotplate for 5 min at 340 °C to activate the passivation and improve the electrical contact. Samples with front surface field (FSF) were processed identically but received an implantation of phosphorus instead of boron on the front side and 10 nm thermal oxide (etched on back side afterwards) instead of $Al_2O_3$.

QSSPC measurements were done with a WCT120 tester. The sheet resistance was determined with a four point probe measurement tool. The doping profiles were measured by electrochemical capacitance-voltage (ECV) profiling. IV curves were measured in house under calibrated standard conditions. Degradation experiments were executed with a sun tester at 500 W/m$^2$.

## 3. Results

### *3.1. Doping profiles & lifetimes*

Figure 1 shows ECV profiles measured after ion implantation of boron or phosphorus and furnace annealing. With the ion implanter used in this study it is possible to run perfectly controlled and uniform processes with doses down to 1e13 ions/cm$^2$ resulting in extremely weak doping profiles with peak doping concentrations in the range of 1e17 to 2e18 cm$^{-3}$. The sheet resistance ($R_{Sheet}$) of the implanted FFE and FSF samples is in the range of several hundred (1e14 cm$^{-2}$ dose) to thousands (1e13 cm$^{-2}$ dose) Ohm per square (see Table 1).

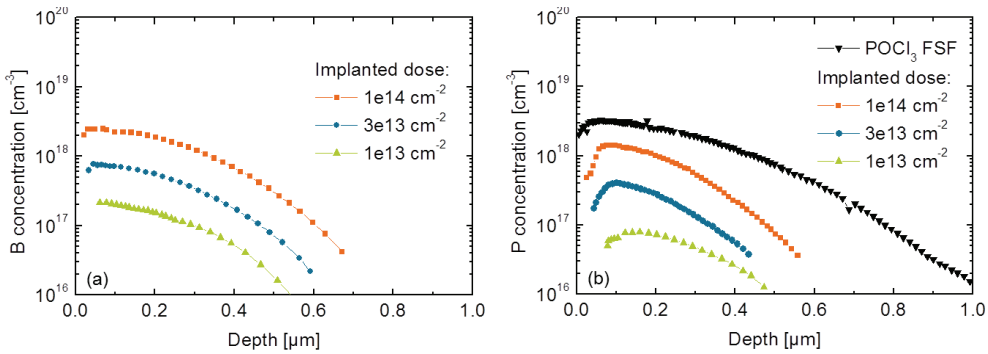


Fig. 1. ECV profiles measured on planar samples after ion implantation and annealing for 80 min at 1050 °C. (a) Low dose boron implantations for a floating emitter; (b) low dose phosphorus implantations for a front surface field. A conventional $POCl_3$-diffused FSF used in Ref [8] is shown for comparison.

The diffusivity of boron and phosphorus during the furnace anneal is quite similar. Profile depths are in the range of 0.5 to 0.7 µm with boron diffusing a little bit deeper. Since the phosphorus profiles are intended for a front surface field passivated by a $SiO_2/SiN_x$ stack, a ~10 nm thick thermal oxide was grown after the annealing. This is done at a much lower temperature and has only a minor influence on the resulting profile, except for the depletion of phosphorus close to the surface.

QSSPC measurements reveal that the saturation current is very low for low dose boron implants passivated with $Al_2O_3$. According to the intended application on the front side of a solar cell, textured samples with random pyramids on both sides have been used for lifetime studies. Saturation current densities ($J_0$) down to 5 fA/cm$^2$ have been achieved (see Table 1). For the boron implanted samples there is a slight trend showing an increase in $J_0$ for higher boron doses. This is because Auger recombination and the surface recombination velocity usually increase with higher doping concentrations (see Ref [9] for $Al_2O_3$). Both effects lead to a higher recombination rate resulting in a higher saturation current. The results of phosphorus implanted samples with $SiO_2/SiN_x$ passivation are also very promising. As can be seen in Table 1, $J_0$ is between 10 and 15 fA/cm$^2$, significantly below the 20 to 25 fA/cm$^2$ measured for the conventional $POCl_3$-diffused FSF profile from Fig. 1b. There is no correlation between phosphorus dose and saturation current. This must be due to the passivation and we assume that the surface recombination velocity, dominating the overall recombination, is weakly influenced by the phosphorus surface concentration for $SiO_2$ on lowly doped *n*-type silicon as it was already simulated by Altermatt *et al*. [10].

Table 1. Characteristics of the investigated profiles (best values achieved so far). Sheet resistance was measured by 4 point probe on planar reference samples. $J_0$ was extracted from QSSPC measurements (textured samples for FSF & FFE and planar samples for emitter and BSF) using the high injection method [11].

| Sample type | Species | Implanted dose [cm$^{-2}$] | $R_{Sheet}$ [Ω/sq] | $J_0$ [fA/cm$^2$] | Passivation |
|---|---|---|---|---|---|
| Floating emitter (FFE) | Boron | 1e13 | 3900 | 5 | $Al_2O_3$ |
| | | 3e13 | 1500 | 6 | |
| | | 1e14 | 650 | 7 | |
| Front surface field (FSF) | Phosphorus | 1e13 | 2200 | 12 | $SiO_2/SiN_x$ |
| | | 3e13 | 880 | 15 | |
| | | 1e14 | 440 | 10 | |
| Emitter | Boron | 7e14 | 147 | 9 | $Al_2O_3$ |
| | | 1e15 | 108 | 22 | |
| | | 1.5e15 | 73 | 24 | |
| Back surface field (BSF) | Phosphorus | 3e15 | 39 | 370 | $Al_2O_3$ |

With boron implantation in the range of 1e15 cm$^{-2}$, an emitter suitable for IBC solar cells can be formed (see Fig. 2a). For the anneal with a high thermal budget applied in this study, the profile depth is around 1 µm with a peak concentration between 1e19 and 3e19 cm$^{-3}$. The sheet resistance ($R_{Sheet}$) can be easily adjusted in the range of 70 to 150 Ω/sq by varying the implanted dose with only small changes of the doping profile. Together with an $Al_2O_3$ passivation we found good electrical properties, i.e. low saturation currents (see Table 1). $J_0$ increases with increasing boron dose, but stays below 30 fA/cm$^2$, even for the highest dose applied (1.5e15 cm$^{-2}$).

For the formation of the phosphorus-doped BSF we investigated a large variety of implanted doses resulting in profiles with sheet resistance ranging from 39 to 240 Ω/sq. Unfortunately, we found a strong injection dependent lifetime for phosphorus surface concentrations around 1e19 cm$^{-3}$ (here, profiles implanted with a dose of 3e14 to 1.5e15 cm$^{-2}$) which makes it impossible to use the high injection method [11] for the extraction of $J_0$ from the lifetime curves. This is most probably due to the fixed negative charge in the $Al_2O_3$ passivation, inappropriate for *n*-doped surfaces [12]. We assume that an injection dependent lifetime will have a negative effect on the fill factor (*FF*) of the solar cell. For the highest phosphorus dose of 3e15 cm$^{-3}$, the high injection method works, giving $J_0$ of 370 fA/cm$^2$. The implied fill factor (*iFF*) extracted from the QSSPC measurement is ~84 % indicating that there are no unusual injection dependent recombination paths. So the *n*-doping seems to dominate over the fixed charges in the passivation. The saturation current of the BSF is quite high, but since the area fraction of the BSF is only around 10 % in the IBC solar cells, the $J_0$ contribution to the whole solar cell is roughly 37 fA/cm$^2$.

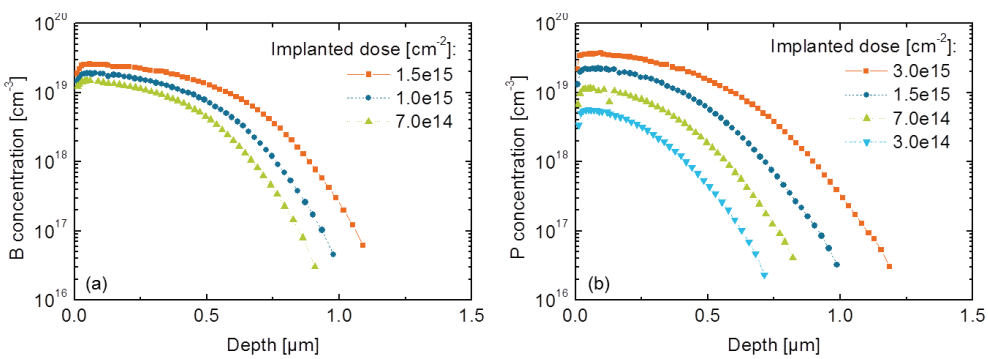


Fig. 2. ECV profiles measured on planar samples after ion implantation and annealing for 80 min at 1050 °C. (a) High dose boron implantations for the emitter; (b) phosphorus implantations for the back surface field.

### 3.2. IBC solar cells

From the investigations on symmetrical lifetime samples we identified useful parameters to fabricate small area IBC solar cells with an industrial contact pitch of 2.1 mm. The structure is schematically shown in Figure 3a. We choose an implantation dose of 1e14 $cm^{-2}$ for front floating emitter (FFE) and front surface field (FSF) because for this process we expect the best process stability and $J_0$ appeared to be very similar for the dose variation investigated in the previous section. 2D simulations of the IBC cell with the data from section 3.1 using COMSOL Multiphysics® predict a better fill factor (*FF*) for a boron emitter with lower sheet resistance at costs of the open-circuit voltage ($V_{OC}$). Since the influence on *FF* is dominant and the overall efficiency should be higher with a stronger boron doping, we applied a boron dose of 1.5e15 $cm^{-2}$ to obtain the emitter with 73 Ω/sq in the solar cell process. The phosphorus BSF was implanted with a dose of 3e15 $cm^{-2}$ (resulting in 39 Ω/sq) to achieve a strong *n*-doping that shows no unusual injection dependent lifetime when being passivated with $Al_2O_3$.

The best solar cell with a boron doped front floating emitter has a conversion efficiency of 21.8 % (see Fig. 3b). With a $V_{OC}$ of 675 mV, the cell is far below of what would be expected from the $J_0$ values measured on lifetime samples. Process references showed that the temperature step applied to the finished cells was not sufficient and the passivation could not be fully activated. Unfortunately, aluminum spikes through the emitter lead to a shunt of the pn junction when the cells were tempered at more than 340 °C. A much higher $V_{OC}$ and cell efficiency should be achievable by activating the passivation prior to the metallization.

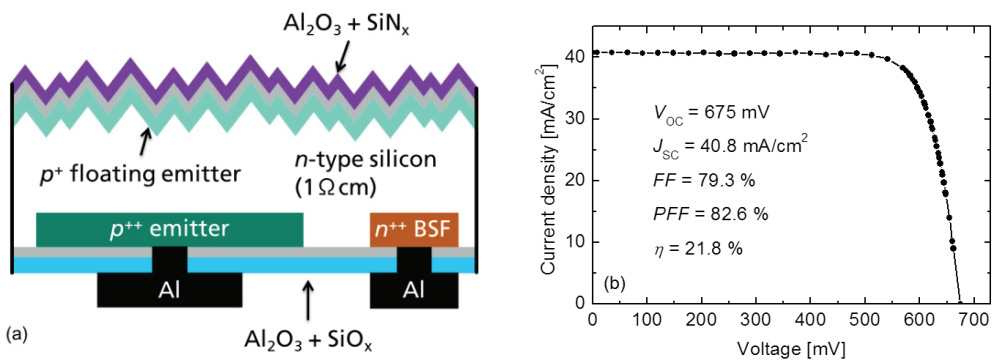


Fig. 3. (a) Cross-sectional sketch of the fabricated IBC solar cells; (b) IV data of the best cell measured in-house. Active cell area is 2 x 2 $mm^2$, thickness is 200 µm, pitch is 2.1 mm.

Degradation experiments were performed in a sun tester with IBC solar cells featuring a front surface field (FSF) passivated by a $SiO_2/SiN_x$ stack or a front floating emitter (FFE) passivated by an $Al_2O_3/SiN_x$ stack. The measurement of IV-data after 36 h exposure to UV-light shows that the cell with FSF degrades strongly, i.e. the current drops to half of its initial value reducing the efficiency from 20.9 to 9.6 % (see Table 2). The cell with FFE is much more stable, but is still losing ~1 % absolute in efficiency. The effect of degradation under UV-illumination has been observed on symmetrical lifetime samples, too. For the FSF, the effective lifetime at a minority carrier density of 1e15 $cm^{-3}$ dropped by 50 to 85 % while the FFE samples remained at an almost constant lifetime level and lost only 2 to 12 %.

It is known that the $SiO_2$ passivation degrades under UV-illumination [5] and Granek *et al*. observed a similar strong degradation of IBC cells but only for cells without front surface field [6]. Note that the overall degradation for the FSF samples shown here is stronger than what has been observed by Granek *et al*., but this might be due to the fact that we used a ~1.5 times higher UV-illumination intensity. The degradation of the cells investigated by Granek *et al*. was efficiently suppressed by using a quite strong doping on the front side (FSF with ~150 Ω/sq) and

explained by the weaker dependence on the surface recombination velocity in case of a FSF underneath the passivation [6]. Hence, we conclude that a weaker FSF which can be formed by ion-implantation as shown in this study in fact enables lower $J_0$ values but becomes more sensitive to the surface passivation quality, especially under UV-illumination.

Table 2. Degradation of IBC solar cells under UV-illumination in a sun tester for 36 h at 500 W/m$^2$.

| Front side | State | $V_{OC}$ [mV] | $J_{SC}$ [mA/cm$^2$] | $FF$ [%] | $\eta$ [%] |
|---|---|---|---|---|---|
| Front surface field (FSF) | before UV exposure | 672 | 39.2 | 79.6 | 20.9 |
| | after UV exposure | 612 | 19.8 | 79.3 | 9.6 |
| Floating emitter (FE) | before UV exposure | 673 | 39.9 | 77.3 | 20.7 |
| | after UV exposure | 668 | 38.2 | 76.7 | 19.6 |

To investigate the cell performance under low level illumination, we measured IV-data with optical filters placed above the solar cells prior to the degradation experiment described above. The resulting illumination intensities were determined by measuring the current of a calibrated reference cell. Those optical filters might have some influence on the spectrum of the incident light, but since we compare two similar cells, this should be of minor importance. In Figure 4 the short-circuit current and open-circuit voltage are plotted against the illumination intensity for a FSF and FFE cell. In both cases the short-circuit current ($J_{SC}$) shows a similar dependence on the amount of incoming photons that can be well described by a linear fit. Neglecting series and parallel resistances, the one-diode equation evaluated at open-circuit conditions

$$J_{SC} = J_0 \times \left( \exp\left( \frac{V_{OC} \cdot q}{n \cdot k_B \cdot T} \right) - 1 \right) \tag{1}$$

with elementary charge $q$, ideality factor $n$, Botzmann constant $k_B$ and temperature $T$ implies a logarithmic dependence of $V_{OC}$ on $J_{SC}$. The logarithmical fit to the measured $V_{OC}$ values in Fig. 4b is a quite good indication that the solar cell performance under low level injection is ideal down to at least 0.01 suns. FSF and FFE show a very similar behavior, not only in $J_{SC}$ and $V_{OC}$ but in $FF$ and efficiency as well (not shown here). This is in contradiction with a former publication where $p$-type IBC cells with a front floating emitter were investigated [7]. Granek *et al.* found a pronounced non-linearity for illumination intensities lower than 0.5 suns and explained this effect by an internal shunt element across the floating junction. It is still unclear whether this effect is present in the $n$-type IBC solar cells fabricated with ion implantation, but if so, it must be much weaker because it is not visible in the IV data down to 0.01 suns shown here.

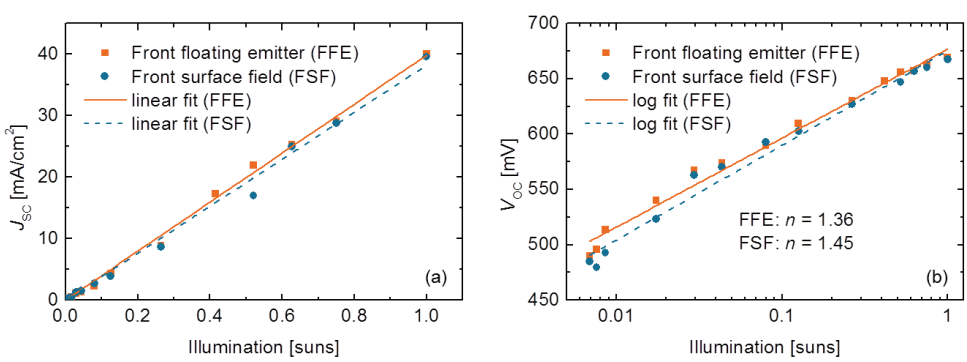


Fig. 4. Comparison of front surface field (FSF) and front floating emitter (FFE) under low level illumination (a) Short-circuit current ($J_{SC}$) with linear fit; (b) Open-circuit voltage ($V_{OC}$) with logarithmic fit corresponding to the one-diode equation.

## 4. Conclusion

Ion implantation is suitable to form lowly doped regions acting as front surface field (FSF) or front floating emitter (FFE) in *n*-type IBC solar cells. Very low saturation current densities ($J_0$) in the range of 10 to 15 fA/cm$^2$ have been achieved for textured FSF samples passivated with a $SiO_2/SiN_x$ stack. These weak profiles strongly depend on the surface recombination velocity and therefore suffer from UV-illumination degrading the $SiO_2$ passivation quality. For textured FFE samples, $J_0$ values down to 5 fA/cm$^2$ were measured with an $Al_2O_3$ passivation. This configuration turned out to be quite stable against UV-irradiation. The sheet resistance of boron emitter and phosphorus BSF can be easily adjusted by the implanted dose. $Al_2O_3$ passivation works well on the boron doped emitter, but for the phosphorus BSF it was found that a surface concentration higher than 3e19 cm$^{-3}$ is necessary to from a suitable BSF and avoid a weird injection dependence of the effective lifetime.

Fully ion implanted and co-annealed IBC solar cells with an $Al_2O_3$ passivation on both sides featuring a weakly boron doped front floating emitter (FFE) were successfully fabricated ($\eta = 21.8$ %). It is known that the $SiO_2$/Si surface recombination velocity increases under UV-illumination [5]. This degradation effect has been identified at lifetime and cell level because the FSF doping used in this study is very weak and therefore very sensitive to the surface passivation. The efficiency of FSF cells dropped dramatically by more than 50% while the FFE cells lost only about 1 % absolute. IV measurements at different illumination intensities revealed a linear dependence of $J_{SC}$ on the injection level for both, FSF and FFE cells. For illumination intensities down to 0.01 suns, no significant influence of an internal shunt element across the floating junction [7] on the IV data was observed.

## Acknowledgements

We want to thank Sonja Seitz, Andreas Lösel, Toni Leimenstoll, Felix Schätzle, Karin Zimmermann and Elisabeth Schäffer for technical assistance and the German Federal Ministry for the Environment, Nature Conservation and Nuclear Safety for founding of this work under contract number 0325292 “ForTeS”.

## References

[1] C.E. Dubé, B. Tsefrekas, D. Buzby, R. Tavares, W. Zhang, A. Gupta, R.J. Low, W. Skinner, J. Mullin, High efficiency selective emitter cells using patterned ion implantation, Energy Procedia 8 (2011) 706-711.
[2] J. Benick, N. Bateman, M. Hermle, Very low Emitter Saturation Current Densities on Ion Implanted Boron Emitters, in: Proceedings of the 25th European PV Solar Energy Conference, Valencia, Spain, (2010).
[3] S. Duttagupta, F.J. Ma, S.F. Lin, T. Mueller, A.G. Aberle, B. Hoex, Progress in surface passivation of heavily doped n-type and p-type silicon by plasma-deposited AlO x/SiNx dielectric stacks, IEEE Journal of Photovoltaics 3 (2013) 1163-1169.
[4] J. Schmidt, A. Merkle, R. Bock, P.P. Altermatt, A. Cuevas, N.-P. Harder, B. Hoex, R. van de Sanden, E. Kessels, R. Brendel, Progress in the surface passivation of silicon solar cells, in: Proceedings of the 23rd European Photovoltaic Solar Energy Conference, Valencia, Spain, (2008).
[5] P.E. Gruenbaum, R.A. Sinton, R.M. Swanson, Light-induced degradation at the silicon/silicon dioxide interface, Applied Physics Letters 52 (1988) 1407-1409.
[6] F. Granek, C. Reichel, Back-contact back-junction silicon solar cells under UV illumination, Solar Energy Materials and Solar Cells 94 (2010) 1734-1740.
[7] F. Granek, M. Hermle, S.W. Glunz Analysis of the current linearity at low illumination of high-efficiency back-junction back-contact silicon solar cells, Physica Status Solidi RRL 2 (2008) 151-153.
[8] C. Reichel, F. Granek, M. Hermle, S.W. Glunz, Back-contacted back-junction n-type silicon solar cells featuring an insulating thin film for decoupling charge carrier collection and metallization geometry, Progress in Photovoltaics: Research and Applications 21 (2013) 1063-1076.
[9] P. Saint-Cast, A. Richter, E. Billot, M. Hofmann, J. Benick, J. Rentsch, R. Preu, S.W. Glunz, Very low surface recombination velocity of boron doped emitter passivated with plasma-enhanced chemical-vapor-deposited AlOx layers, Thin Solid Films 522 (2012) 336-339.
[10] P.P. Altermatt, J.O. Schumacher, A. Cuevas, S.W. Glunz, R.R. King, G. Heiser, A. Schenk, Numerical modeling of highly doped Si:P emitters based on Fermi-Dirac statistics and self-consistent material parameters, Journal of Applied Physics 92 (2002) 3187-3197.
[11] D.E. Kane, R.M. Swanson, Measurement of the emitter saturation current by a contactless photoconductivity decay method (silicon solar cells), in: Proceedings of the 18th IEEE Photovoltaic Specialists Conference, Las Vegas, Nevada, USA, (1985).
[12] B. Hoex, M.C.M. van de Sanden, J. Schmidt, R. Brendel, W.M.M. Kessels, Surface passivation of phosphorus-diffused $n^+$-type emitters by plasma-assisted atomic-layer deposited $Al_2O_3$, Physica Status Solidi RRL 6 (2012) 4-6.